Journal of Engineering Mathematics, Vol. 15, No. 4, October 1981

©1981 Sijthoff & Noordhoff International Publishers – Alphen aan den Rijn
Printed in the Netherlands

Injection from a finite section of a flat plate placed parallel to a uniform stream

F. T. SMITH

Mathematics Department, Imperial College, London SW7 2BZ, U.K.

and

S. C. R. DENNIS

Applied Mathematics Department, University of Western Ontario, London, Canada N6A 5B9

(Received November 11, 1980)

SUMMARY

A study is made of the effects on the fluid motion past a semi-infinite flat plate of introducing a uniform injection of extra fluid from a finite porous section of the plate. Steady laminar flow is considered with a uniform oncoming stream parallel to the plate in an incompressible fluid. A local analysis valid near the start and finish of the injection is found to produce unusually firm predictions for the singular behaviour of the solution of the Navier-Stokes equations there and in particular shows that separation ahead of the injection is inevitable for all positive Reynolds numbers R. Then a numerical treatment of these singular points, and of the Navier-Stokes equations and boundary conditions, is described and the results are presented for a range of values of R. The calculation method used is based on the accurate and efficient centred differencing technique suggested by Dennis [1] and developed recently by Dennis and Hudson [2]. Checks on the influences of mesh spacing, of the placing for the outer boundaries of the computational domain, and of the treatments of the singular points are given. The agreement found with the previous local analysis near the ends of the injection proves especially encouraging. In addition the results provide some guidance to the asymptotic structure of the flow at high Reynolds numbers and to the questions surrounding the occurrence of large-scale separations.

1. Introduction

The theoretical and practical effects on the fluid motion past a fixed surface of allowing extra fluid to be injected through a porous section of the surface have been the subjects of study for many years. The usual applications in mind have been within the context of aerodynamics, where for example injection is used in the jet-flap configuration at or near the trailing edge of an aerofoil (Spence [3], [4], Stratford [5], [6], Leamon and Plotkin [7], Sato [8], Ives and Melnik [9], O'Mahoney and Smith [10]) or within the context of internal flow dynamics where fluid injection is often intended to act as a coolant for a turbine blade (for instance, Hartunian and Spencer [11], [12], Fernandez and Zukoski [13]). One of the main practical reasons for investigating the effects of injection is the possibly disadvantageous influence that injection can exert especially on boundary layer transition, control and/or separation at high Reynolds num-

bers. This has to be compared with the advantages to be gained from the intended cooling of the surface or the increase in lift desired. The methods and aims in the vast number of studies that have been made of fluid injection phenomena differ widely and include experimental, numerical and theoretical works on both laminar and turbulent flow, in two- or three-dimensional internal or external flow situations. Both compressible and incompressible fluid flow properties have been considered. Reviews and references on the subject have been given by Goldstein [14], Inger and Gaitatzes [15] and Smith and Stewartson [16], among others.

Given this great diversity of interest in injection problems we shall confine our attention henceforth largely to steady laminar two-dimensional external flows with injection, for the sake of brevity. The relevant theoretical work then has mainly been concerned with attempting to predict the basic features of the motion in the most important practical regime of high Reynolds number flows, starting with Pretsch's [17] study of the boundary layer response to a relatively weak amount of injection. A common approach has been to seek similarity solutions, following Emmons and Leigh's [18] calculations of the Falkner-Skan problem with injection. Unfortunately such solutions generally require the presence of unrealistic distributions of injection at the surface, often with a semi-infinite length assumed for the porous section (although some exceptions to this are mentioned and investigated by Diver and Stewartson [19]). Indeed, if we concentrate on the probably most realistic theoretical distribution, that of uniform injection from a porous section of finite length, then the number of relevant papers is reduced considerably. All are concerned in fact with the injection of fluid from a finite porous section of a flat plate in a uniform stream. First, Catherall, Stewartson and Williams [20] considered the case of weak injection starting at the leading edge of the plate, integrated the boundary layer equations up to the onset of separation and there examined in detail the structure of the nearly separated flow. Next, Smith [21] and Smith and Stewartson [16] studied the supersonic slot-injection problem for stronger injection from a small porous slot situated downstream from the leading edge. Using triple-deck theory (see Stewartson [23], Messiter [24]) they obtained analytical and numerical results for the ensuing flow solutions including some with separation occurring near the start of the injection. The latter then provided the basis for the analysis by Smith [21], Smith and Stewartson [22] and Stewartson [25] of the motion due to strong injection from a porous section whose length is not small. There, for supersonic flow, separation of the Stewartson and Williams [26] form is predicted to occur well ahead of the start of the injection and an apparently complete asymptotic description of the flow field proves attainable. This is to be contrasted with the asymptotic descriptions of other related external supersonic flow problems involving separation (Messiter, Hough and Feo [27], Burggraf [28], [29]) where due to difficulties concerning the subsequent reattachment process downstream the theory remains not quite complete.

The injection problem above therefore stands out as the one problem involving separation for which a complete asymptotic account has been given, at least in supersonic flow. In subsonic flow earlier attempts had been made by Wallace and Kemp [30] and Smith [21], [31] to provide an account for the asymptotic flow properties with strong injection, but these attempts were of a tentative nature. They were based on the Cole and Aroesty [32] model for strong injection and in particular did not allow for any significant upstream separation, which is implied by analogy with the supersonic flow solution of Smith and Stewartson [22] and is governed presumably by the Sychev [33]-Smith [34] theory for subsonic separation. Further attempts by

Drs. F. T. Smith and P. W. Duck aimed at handling the theoretical subsonic description for high Reynolds number flow are under way, however. Again the hope is that as for the supersonic case a complete description will be forthcoming, including an adequate resolution of the re-attachment process which in other related subsonic flow problems with separation (Smith [35]) causes difficulties very similar to those arising in the related supersonic flow problems described in the previous paragraph. Experimentally there is some evidence, in subsonic (Smith [31]) as well as supersonic conditions (Hartunian and Spencer [11], [12], Fernandez and Zukoski, [13]) to support the view that separation does occur significantly far ahead of the injection in laminar or turbulent flow at high Reynolds numbers. By contrast, however, numerical solutions of the subsonic triple-deck problem for slot-injection calculated by Napolitano and Messick [36] (see also Smith [21]) tend to suggest the occurrence of a much more significant separation downstream of the porous section. To date therefore the asymptotic account of the primary effects of injection is far from clear in subsonic flow.

An alternative theoretical approach to the problems associated with fluid injection in subsonic flow is to seek numerical solutions of the Navier-Stokes equations for finite values of the Reynolds number. As far as we know there has been little or no concerted effort made on this aspect of the flow problems. Accordingly in this paper we will address the basic problem of injection from a finite porous section of a semi-infinite flat plate placed parallel to a uniform oncoming stream and we will describe a numerical treatment and solution of the Navier-Stokes equations for a range of values of the Reynolds number. It is assumed that the fluid is incompressible and that the flow remains steady, laminar and two-dimensional throughout. Some of the initial aims of the computational approach here are to provide quantitative information on the resultant flowfield for finite values of the Reynolds number, thereby to judge the relevance of *inter alia* the asymptotic proposals mentioned above for high Reynolds numbers and hopefully even to provide some further guidance for the asymptotic theory. The last objective here is given some credence by the recent calculations of Dennis and Smith [37] for separating flow through a channel with a step. They found very good agreement with the corresponding asymptotic theory of Smith [38] for Reynolds numbers of the order of 100 or greater. During the course of the present work it turns out however that another significant objective can also be set: namely, the testing of the accuracy of the numerical approach near known singularities of the flow solution. For an analysis of the solution of the Navier-Stokes equations near the start or finish of the injection yields certain irregular properties that ideally should be reproduced in any numerical treatment. Moreover these properties, obtained from an extension of the Dean-Montagnon [39] and Moffatt [40] theory, do not contain the high degree of arbitrariness which is usually associated with such local analyses. So an unusually firm comparison can be made locally with any numerical solution of the full injection problem.

The governing equations and boundary conditions are set out in Sec. 2 below together with the local analysis for the irregular properties of the problem near the ends of the injection. This analysis also confirms two main attributes of the solution for finite values of the Reynolds number. First, separation, or flow reversal, is bound to occur ahead of the injection since the wall vorticity is infinitely positive at the starting point of the injection. Second, the fluid must certainly be forward-moving sufficiently close to the finish of the injection since at the finishing point the wall vorticity is infinitely negative.

The numerical approach adopted for the Navier-Stokes equations is described in Sec. 3 and

is based on the efficient centred differencing scheme proposed by Dennis [1] and developed by Dennis and Hudson [2]. The treatment of the boundary conditions is also described in Sec. 3. Then Sec. 4 presents the main numerical solutions obtained and the results of the tests applied to them. In particular the comparisons with the local properties predicted in Sec. 2 prove fairly encouraging. The possible implications for high Reynolds number flows, including the question of the position of the separation point ahead of the injection, are also discussed in Sec. 4. Further comments are made in Sec. 5.

2. The governing equations and certain local properties

The situation to be considered concerns the steady laminar two-dimensional flow of an incompressible fluid past a semi-infinite flat plate, a finite section of which is porous (Figure 1). The plate, given by $y^* = 0$, $x^* > 0$ in cartesian coordinates x^*, y^*, is aligned with a uniform free stream of speed U_∞^* at infinity upstream and the porous section $y^* = 0$, $x_s^* < x^* < x_F^*$, say, of the plate allows a uniform normal injection of the same fluid at a given speed V_W^*. Here $x_s^* > 0$, $V_W^* \geqslant 0$. The motion is assumed to be symmetric about $y^* = 0$, so that only the upper half plane $y^* \geqslant 0$ needs to be considered. A suitable definition of the Reynolds number is

$$R = 2U_\infty^* x_s^*/\nu^* \tag{2.1}$$

where ν^* is the kinematic viscosity of the fluid. Hence with the nondimensional coordinates $(x, y) = (x^*, y^*)/2x_s^*$ and corresponding velocity components u, v nondimensionalized with respect to U_∞^*, the Navier-Stokes equations take the form

$$\begin{aligned} &R(\psi_y \zeta_x - \psi_x \zeta_y) = \nabla^2 \zeta, \\ &\zeta = -\nabla^2 \psi \end{aligned} \tag{2.2}$$

where $\nabla^2 \equiv \partial^2/\partial x^2 + \partial^2/\partial y^2$ and ζ, ψ give the vorticity and stream function, so that

$$u = \psi_y, \quad v = -\psi_x. \tag{2.3}$$

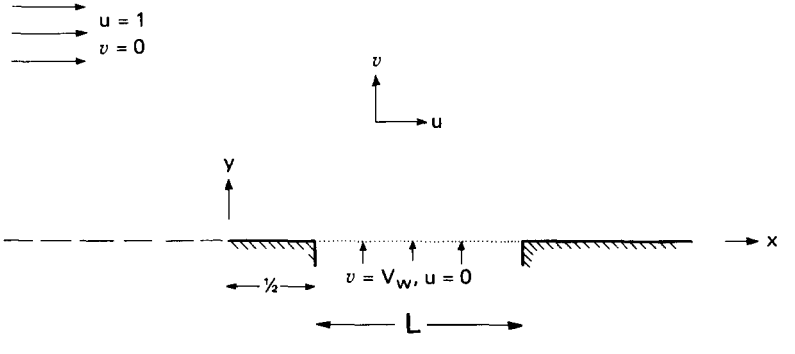

Figure 1. Sketch of the nondimensionalized flow problem and the coordinate system.

The boundary conditions at $y = 0$, upstream of and along the plate, require

$$\text{at } y = 0 \quad \begin{cases} \psi = \zeta = 0 & \text{for } x < 0, \quad (2.4a) \\ \psi = 0, \quad \psi_y = 0 & \text{for } 0 < x < 1/2, \quad (2.4b) \\ \psi = -V_w(x - 1/2), \quad \psi_y = 0 & \text{for } 1/2 < x < L + 1/2, \quad (2.4c) \\ \psi = -V_w L, \quad \psi_y = 0 & \text{for } x > L + 1/2 \quad (2.4d) \end{cases}$$

for symmetry and for the no-slip or injection constraints, along the plate. Here $V_w = V_w^*/U_\infty^*$ and $L = (x_F^* - x_s^*)/2x_s^*$ are given finite parameters representing the relative speed and length of the normal injection. The free-stream conditions impose the constraints

$$\psi_y \to 1, \quad \psi_x \to 0 \quad \text{as } x^2 + y^2 \to \infty \text{ generally}, \tag{2.5}$$

although we must allow for the eventual emergence of a boundary layer-like flow at downstream infinity. There the effect of the injection diminishes and to *leading* order the motion is expected to approach the Blasius form appropriate to motion past an impermeable semi-infinite flat plate. Thus as $x^2 + y^2 \to \infty$ but with $y/x^{1/2}$ fixed (2.5) is replaced by the asymptote

$$\psi \sim x^{1/2} f_B(R^{1/2} y/x^{1/2}) \tag{2.6}$$

where f_B is the Blasius function satisfying $2f_B''' + f_B f_B'' = 0$, $f_B(0) = f_B'(0) = 0$, $f_B'(\infty) = 1$.

Our numerical treatment of the governing equations (2.2) with the constraints (2.4)-(2.6) is discussed in Sec. 3 below. Beforehand certain local properties of the solution are worthy of examination. First, near the leading edge $x = y = 0$ of the plate the solution is expected to approach a well-known classical form, associated also with the motion past an impermeable flat plate, in which the stream function ψ is proportional to the 3/2th power of distance from the leading edge. Therefore the vorticity ζ is singular there, being proportional to the inverse 1/2th power of that distance (see Dean and Montagnon [39], Moffatt [40], Walsh [41] and others). The second local property concerns the solution near the start of the injection at $x = 1/2$. There an analysis similar to that of Moffatt [40] can be applied and provides some surprisingly fruitful results. After some trial and error, and bearing in mind the corresponding results for zero injection [40], we reach the conclusion that the solution expands locally in the form

$$\begin{aligned} \psi &= r f_0(\theta) + r^2 \ln r f_{1L}(\theta) + r^2 f_1(\theta) + \ldots, \\ -\zeta &= r^{-1} F_0(\theta) + \ln r F_{1L}(\theta) + F_1(\theta) + \ldots \end{aligned} \tag{2.7}$$

where

$$x - 1/2 = r\cos\theta, \quad y = r\sin\theta \quad \text{and} \quad 0 < r \ll 1.$$

Substituting (2.7) into (2.2) and equating terms of equal order in r yields the typical slow-flow equations

$$F_0'' + F_0 = 0, \quad F_0 = f_0'' + f_0 \tag{2.8a}$$

at leading order, while the boundary conditions (2.4b, c) require

$$f_0(0) = -V_W, \; f_0'(0) = f_0(\pi) = f_0'(\pi) = 0. \tag{2.8b}$$

From (2.8a, b) we obtain the leading order terms

$$f_0(\theta) = V_W \pi^{-1} (\theta \cos\theta - \sin\theta - \pi \cos\theta), \tag{2.8c}$$

$$F_0(\theta) = -2 V_W \pi^{-1} \sin\theta, \tag{2.8d}$$

the streamlines for which are shown in Figure 2. Notice however that, at $\theta = 0, \pi$, (2.8d) gives no contribution to the behaviour of the wall vorticity $\zeta(x, 0)$ near the start of the injection. Instead we must proceed to the second-order terms in the local solution which are governed by a slow-flow equation again,

$$f_{1L}^{iv} + 4 f_{1L}'' = 0,$$

from (2.2) and (2.7), and by $f_{1L} = f_{1L}' = 0$ at $\theta = 0, \pi$. Hence

$$f_{1L} = A_L (\cos 2\theta - 1); \quad F_{1L} = -4 A_L \tag{2.9}$$

where A_L is a constant as yet unknown. However, A_L can be determined from the third-order terms of (2.7) which from substitution into (2.2) satisfy

$$f_1^{iv} + 4 f_1'' = -4 f_{1L}'' - R(f_0 F_0)' \tag{2.10a}$$

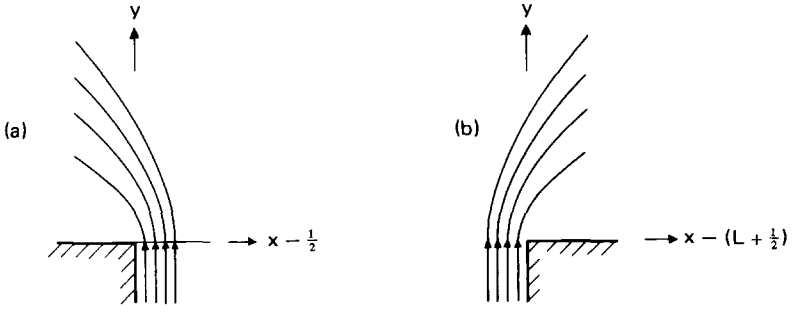

Figure 2. (a) The streamlines near the start of the injection at $x = 1/2$ according to the leading term of the local prediction (2.7) (see also (2.8c)). (b) The corresponding streamlines near the finish of the injection at $x = L + \frac{1}{2}$.

and the boundary conditions

$$f_1 = f_1' = 0 \quad \text{at} \quad \theta = 0, \pi \tag{2.10b}$$

from (2.4b, c). It is noteworthy that (2.10a) marks the first appearance of the nonlinear inertial effect ($\propto R$ in (2.2)) on the expansion and that the presence of the logarithmic term f_{1L} is necessary to counteract the inertial effect in (2.10a) and to allow (2.10a, b) to be soluble. The solution of (2.10a) is

$$f_1 = A_1 \cos 2\theta + B_1 \sin 2\theta + C_1 \theta + D_1$$
$$+ E_1 \theta \cos 2\theta + G_1 \theta \sin 2\theta + H_1 \theta^2 \sin 2\theta \tag{2.11a}$$

where the constants A_1, B_1, C_1, D_1 remain unknown but E_1, G_1, H_1 are given by

$$8G_1 = 8A_L + RV_W^2 \pi^{-1}, \; 16H_1 = -RV_W^2 \pi^{-2}, \; 16E_1 = 40H_1 - RV_W^2 \pi^{-2} \tag{2.11b}$$

because of (2.8c, d), (2.9). Applying (2.10b) then requires

$$A_1 + D_1 = 0; \quad B_1 = 0;$$
$$C_1 + E_1 = 0; \quad G_1 = -H_1 \pi. \tag{2.11c}$$

The last equation here, along with (2.11b), fixes the value of A_L and we find

$$A_L = -RV_W^2/16\pi. \tag{2.12}$$

Hence putting $\theta = 0, \pi$ in (2.7) and using (2.9), (2.12) we have the leading-order nonzero terms

$$\zeta_W \sim -\frac{RV_W^2}{4\pi} \ln |x - \tfrac{1}{2}| + O(1) \tag{2.13}$$

for the wall vorticity near $x = 1/2\pm$. The $O(1)$ term in (2.13) is proportional to A_1 in fact but A_1 is not fixed by (2.11c), or presumably by the local expansion at all, but remains an unknown to be fixed by the global solution of our flow problem. Local properties similar to those above hold also near the finish of the injection at $x = L + 1/2$ and are referred to later in Sec. 4.

An unusual feature of the local forms in (2.7) above is their lack of arbitrariness in the two dominant pairs (f_0, F_0) and (f_{1L}, F_{1L}) of the expansions; the arbitrariness inherent in any local expansion is here suppressed until the third pair (f_1, F_1) in (2.7), wherein the constant A_1 first appears. Since, clearly, some special treatment is called for to take satisfactory account of the irregular nature of the solution near the start and finish of the injection, as well as near the leading edge, the analytical results (2.8c, d), (2.13) in particular and their counterparts near the finish of the injection provide valuable checks on the accuracy of any such special treatment adopted. The relevant comparisons between (2.8c, d), (2.13) and our numerical results are

presented in Sec. 4 below, after the description in Sec. 3 of the numerical approach used for the solution of (2.2)-(2.6) and for the treatment of the three singular points $(x, y) = (0, 0)$, $(1/2, 0)$, $(L + 1/2, 0)$.

Two final significant points about the local forms in (2.7)-(2.13) are that they show the inevitability of separation occurring ahead of the injection and that correspondingly there is a strongly attached flow occurring in the neighbourhood of the finish of the injection. The local streamlines drawn in Figure 2 demonstrate this facet and although the wall vorticity associated with those streamlines happens to be zero, the next-order term (see (2.13)) in the local expansion of the wall vorticity confirms the presence next to the plate of reversed flow sufficiently close to the start of the injection, since $-\zeta_W < 0$ there. Similarly, the counterpart of (2.13) near $x = L + 1/2$ confirms the presence next to the plate of forward motion near the finish of the injection, with $-\zeta_W > 0$ there. Therefore the important question of *whether* flow reversal occurs upstream of the injection or not, for a given Reynolds number, does not have to be left to a full numerical attack on the Navier-Stokes problem (2.2)-(2.6). Rather, the local analysis alone firmly predicts the existence of upstream flow reversal at all nonzero Reynolds numbers and the full numerical solution of (2.2)-(2.6) then has to settle *where* the flow reversal upstream occurs at each particular Reynolds number considered.

3. The numerical approach

To account for the singular nature of the solution both near the leading edge and in the far downstream form (2.6) the flow field, the upper half of the x-y plane, can be mapped conformally to the positive quadrant of an ξ-η plane defined by

$$x + iy = \frac{1}{2}(\xi + i\eta)^2, \tag{3.1}$$

as in Walsh [41]. This has the advantage that the local form near the leading edge $\xi = \eta = 0$ and the far downstream behaviour (2.6) as $\xi \to \infty$ both become dependent on ξ, η rather than on $x^{1/2}, yx^{-1/2}$. The governing equations become

$$R(\psi_\eta \zeta_\xi - \psi_\xi \zeta_\eta) = \tilde{\nabla}^2 \zeta, \tag{3.2a}$$

$$J\zeta = -\tilde{\nabla}^2 \psi \tag{3.2b}$$

where $J \equiv \xi^2 + \eta^2$, $\tilde{\nabla}^2 \equiv \partial^2/\partial\xi^2 + \partial^2/\partial\eta^2$, while the boundary conditions are now

$$\psi = \zeta = 0 \quad \text{at} \quad \xi = 0 \quad \text{for} \quad \eta > 0; \tag{3.3a}$$

$$\text{at } \eta = 0, \begin{cases} \psi = 0, \quad \psi_\eta = 0 & \text{for } 0 < \xi < 1, \quad (3.3b) \\ \psi = -\tfrac{1}{2} V_W(\xi^2 - 1), \quad \psi_\eta = 0 & \text{for } 1 < \xi < (2L+1)^{1/2}, \quad (3.3c) \\ \psi = -V_W L, \quad \psi_\eta = 0 & \text{for } \xi > (2L+1)^{1/2} \quad (3.3d) \end{cases}$$

from (2.4a-d); and

$$\psi_\eta \to \xi, \quad \zeta \to 0 \quad \text{as} \quad \eta \to \infty \text{ with } \xi \text{ fixed}, \tag{3.4}$$

$$\psi \sim 2^{-1/2}\, \xi f_B(2^{1/2}\eta) \text{ as } \xi \to \infty \text{ with } \eta \text{ fixed} \tag{3.5}$$

from (2.5), (2.6) respectively.

In our numerical treatment the discretization of the Navier-Stokes equations (3.2a, b) is performed in a manner similar to that of Dennis and Hudson [2] and Dennis and Smith [37], following Dennis' [1] suggestion. A uniform rectangular mesh with M lines parallel to the ξ-axis and N lines parallel to the η-axis is used to span the finite ranges $0 \leqslant \xi \leqslant \xi_\infty$, $0 \leqslant \eta \leqslant \eta_\infty$, replacing the infinite ranges $(0, \infty)$ in ξ, η in (3.2)-(3.5). Here $\xi_\infty = (M-1)h$, $\eta_\infty = (N-1)h$ where h is the mesh width, and M, N are chosen so that the start and finish of the injection, at $\xi = 1$, $(2L+1)^{1/2}$ with $\eta = 0$, are mesh points. Then (3.2b) is replaced by the centred difference approximation

$$-h^2 (J\zeta)_0 = \psi_1 + \psi_2 + \psi_3 + \psi_4 - 4\psi_0, \tag{3.6}$$

nominally of second-order accuracy in h, in the usual way. Here the subscripts 0, 1, 2, 3, 4 refer to evaluation at the points (ξ_0, η_0), $(\xi_0 + h, \eta_0)$, $(\xi_0, \eta_0 + h)$, $(\xi_0 - h, \eta_0)$, $(\xi_0, \eta_0 - h)$ respectively, where $(\xi_0, \eta_0) = (mh, nh)$ is a typical internal meshpoint so that $1 \leqslant m \leqslant M-2$, $1 \leqslant n \leqslant N-2$. For reasons of iterative convergence, however, (3.2a) is replaced by the augmented central-difference approximation

$$\begin{aligned} &\left[1 - \frac{1}{2} Rh\bar{u}_0 + \frac{1}{8} (Rh\bar{u}_0)^2\right]\zeta_1 + \left[1 - \frac{1}{2} Rh\bar{v}_0 + \frac{1}{8} (Rh\bar{v}_0)^2\right]\zeta_2 \\ &+ \left[1 + \frac{1}{2} Rh\bar{u}_0 + \frac{1}{8} (Rh\bar{u}_0)^2\right]\zeta_3 + \left[1 + \frac{1}{2} Rh\bar{v}_0 + \frac{1}{8} (Rh\bar{v}_0)^2\right]\zeta_4 \\ &\qquad = \left[4 + \frac{1}{4} (Rh)^2 (\bar{u}_0^{\,2} + \bar{v}_0^{\,2})\right]\zeta_0 \end{aligned} \tag{3.7}$$

where $\bar{u}_0 = (\psi_2 - \psi_4)/2h$, $\bar{v}_0 = (\psi_3 - \psi_1)/2h$. The five terms proportional to $(Rh)^2$ in (3.7) would be missing in the standard central-difference approximation of course but their inclusion here, as explained by Dennis and Hudson [2] and Dennis and Smith [37], helps to overcome the difficulty associated with loss of diagonal dominance in the standard difference equations particularly at higher Reynolds numbers. Indeed, diagonal dominance is assured for all Reynolds numbers by the presence of those five extra terms. Moreover they do not alter the second-order accuracy of the central-difference approach. Like (3.6), (3.7) is applied at all internal mesh points ξ_0, η_0 except for the two special points where $\eta_0 = h$ with $\xi_0 = 1$ or $\xi_0 = (2L+1)^{1/2}$. There the momentum equation (3.7) as it stands would require use of the value of the wall vorticity ζ_W at the start and finish of the injection, which is undesirable in view of *inter alia* the logarithmic singularity in ζ_W there according to (2.13). To avoid reference to the wall vorticity at those two points alone we use differencing in the $\xi - \eta$ and $\xi + \eta$ directions instead of in the

ξ and η directions of (3.7). Once again, the nominal second order accuracy of the scheme is preserved. A similar special treatment is not required for (3.6) incidentally because the stream function near the start and finish of the injection is not singular and in fact is only weakly irregular (see Sec. 2). It is worth observing also that the transformation from the x–y half plane to the ξ–η quarter plane permits the singular point at the leading edge to be bypassed automatically by the internal difference equations (3.6), (3.7). Tests on the adequacy of these treatments of the three singular points $\xi = 0, 1, (2L+1)^{1/2}$ on the plate are described below.

The symmetry conditions (3.3a) are applied by setting ψ, ζ equal to zero at $\xi = 0$, $\eta = mh$ for $1 \leqslant m \leqslant M-1$, throughout, while the boundary conditions on ψ in (3.3b-d) are set at $\eta = 0$ for $\xi = (n-1)h$ with $1 \leqslant n \leqslant N$. The boundary conditions on ψ_η in (3.3b-d) are maintained by means of the difference formulation

$$J_0\zeta_0 = -\frac{3}{2h^2}(\psi_1 + 2\psi_2 + \psi_3 - 4\psi_0) - \frac{1}{2}J_2\zeta_2 \tag{3.8}$$

stemming from Woods' [42] approach. Similarly the outer boundary conditions in (3.4) are replaced by the constraints

$$\zeta_0 = 0, \quad 4\psi_0 = \psi_1 + \psi_3 + 2\psi_4 + 2h\xi + \frac{h^2}{3}\zeta_4 J_4. \tag{3.9}$$

In the constraints (3.8) and (3.9) the suffices 0, 1, 2, 3, 4 are defined as for (3.6), (3.7), with $1 \leqslant n \leqslant N-2$ but $m = 1$ in the case of (3.8) and $m = M$ for (3.9). Both the constraints are second order accurate and link the boundary values of ψ, ζ with the nearest local internal values of ψ, ζ.

Finally, it was decided that the treatment of the asymptotic downstream condition (3.5) would have to account satisfactorily for the difficulty concerning the unknown origin shift implicit in (3.5). A seemingly acceptable way of doing so is to insist that the flow acquires a boundary layer-like form at the downstream extremity of the integration range. Thus it is supposed that the operator $\partial/\partial\xi$ is negligible then compared with $\partial/\partial\eta$, so that the downstream constraint becomes

$$\left[2 + \frac{1}{2}R(\psi_2 - \psi_4)\right]\zeta_0 = \left[1 + \frac{1}{2}R(\psi_0 - \psi_3)\right]\zeta_2 + \left[1 - \frac{1}{2}R(\psi_0 - \psi_3)\right]\zeta_4 + \frac{1}{2}R(\psi_2 - \psi_4)\zeta_3, \tag{3.10a}$$

$$\psi_0 = \frac{1}{2}\left[\psi_2 + \psi_4 + h^2 J_0\zeta_0\right] \tag{3.10b}$$

where the suffices 0, 2, 3, 4 are as for (3.6), (3.7) but with $n = N-1$ for $1 \leqslant m \leqslant M-2$. Backward differencing in ξ has also been applied, in obtaining (3.10a,b), to reflect the expected parabolic nature of the far downstream boundary layer flow. The loss of accuracy in approximating in backward differences the far downstream form here is not expected to reduce the accuracy of the majority of the flow solution at all significantly, although tests on its effect will be described later, in Sec. 4. The boundary layer equations (3.10a, b) are regarded as con-

sistency relations between the values of the solutions at the last two meshlines $\xi = \xi_\infty - h, \xi_\infty$.

The Gauss-Seidel iterative procedure used to solve (3.6)-(3.10) was similar to that of Dennis and Smith [37] and others. Given a complete guess for ψ, ζ and with the boundary conditions on ψ, ζ at $\xi = 0$, on ζ at $\eta = \eta_\infty$ and on ψ at $\eta = 0$ set throughout, (3.7) was used to update the interior ζ field, following which (3.10a) gave the new values of ζ at $\xi = \xi_\infty$ while (3.9) enabled the recalculation of ψ at $\eta = \eta_\infty$. Then (3.6) was used to update the interior ψ field (except at the two special points mentioned before) followed by (3.10b) which fixed the new values of ψ at $\xi = \xi_\infty$ and (3.8) which fixed the new values of the wall vorticity. This enabled (3.7) to be re-solved and so the iteration continued. No relaxation was applied to the recalculation of the boundary values of ζ and ψ in (3.8) and (3.9) respectively but some over-relaxation was used occasionally in the iterative solution of (3.6) and (3.7). Starting guesses for ψ, ζ were provided by the uniform stream solution $\psi = \xi_\eta, \zeta = 0$ supplemented by the known boundary values of ψ at $\eta = 0$. The convergence criterion imposed was that two successive iterative sweeps should yield values of ζ sufficiently close everywhere that the sum, over the computational field, of the absolute values of the changes in ζ at every point should be less than 0.0005. The criterion was enough in practice to ensure that the numerical solutions for the wall vorticity ζ_W in particular were known to at least four significant figures.

The effects of the discretization of the governing equations and the boundary conditions including the special points mentioned above were examined in detail and are discussed in the next section. Tests on the influence of the mesh spacing h in the equations and boundary conditions were made by completing solutions for different values of h and inspecting the resulting differences. With regard to the two special points at the start and finish of the injection comparisons were made between our calculated solutions and the local theory of (2.7)-(2.13) near $\xi = 1$ and its counterpart near $\xi = (2L + 1)^{1/2}$. The effect of the other special point, the leading edge, was tested by obtaining a solution with zero injection ($V_W = 0$) so that comparisons could be made with the corresponding solutions of other workers who used different approaches. Lastly the effect of the curtailment of the integration range at $\xi = \xi_\infty$ and $\eta = \eta_\infty$ was investigated by calculating and comparing numerical solutions for different values of ξ_∞, η_∞ with a fixed mesh spacing h.

4. Numerical results

We present first, in Figure 3, the numerical solution obtained for the wall vorticity ζ_W in the case of zero injection, $V_W = 0$, using a mesh width $h = 1/20$ and outer boundaries $\xi_\infty = 8, \eta_\infty = 4$ so that along the x-axis the computational domain extended from $x = -8$ to $x = 32$. Also shown for the purpose of comparison is the numerical solution of Walsh [41]. The agreement between the two seems fairly encouraging and tends to support our treatment of both the leading edge singularity and the farfield conditions, as well as suggesting that the mesh width $h = 1/20$ gives reasonably accurate solutions. Walsh's [41] results in turn agree quite well with those of Van de Vooren and Dijkstra [43] and Van de Vooren and Veldman [44] for this classical problem of the flow past an aligned impermeable semi-infinite flat plate.

The remaining solutions for nonzero injection were all obtained with the injection velocity $V_W = 0.2$ and injection length $L = 1.5$ so that the injection starts at $\xi = 1$ and finishes at $\xi = 2$.

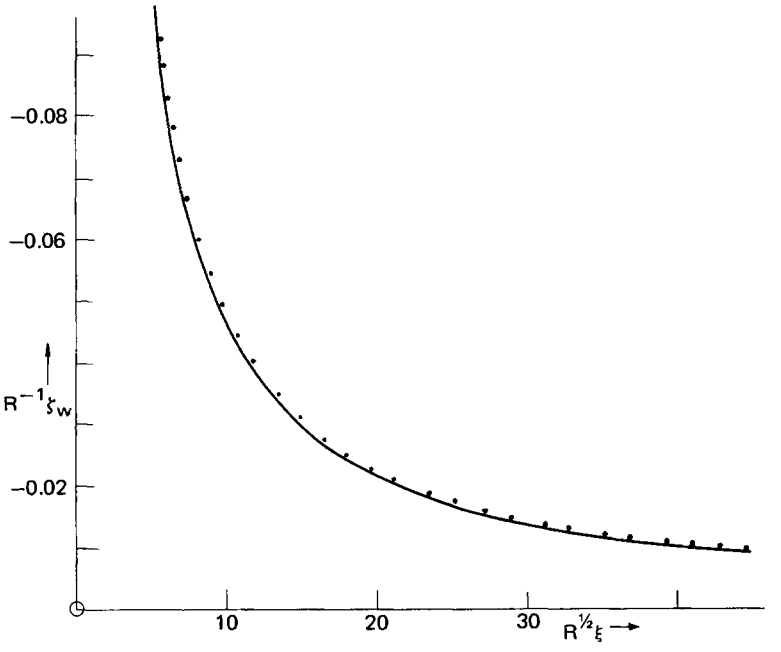

Figure 3. Numerical solutions (for any $R > 0$) for the wall vorticity ζ_W versus $\xi = \frac{1}{2}x^2$ for the case of the impermeable wall where $V_W = 0$. ——, present calculations; ····, from Walsh [41].

The solutions for the wall vorticity ζ_W as a function of $\xi = (2x)^{1/2}$ are shown in Figure 4 (a)-(d) for the four Reynolds numbers R = 1, 10, 50, 100. For the three lowest Reynolds numbers numerical solutions were calculated for two different mesh widths, h = 1/10, 1/20 while at the highest Reynolds number R = 100 solutions for the three mesh widths h = 1/10, 1/20, 1/30 were obtained, along with a solution for an increased range of integration. The effect of decreasing the value of h seems to be a fairly regular phenomenon throughout. In particular, for R = 100 the closeness of the solutions for h = 1/20 and h = 1/30 in Figure 4(d) suggests strongly that h^2 extrapolation on the results from the two meshes with h = 1/10, 1/20 is quite justifiable. The same conclusion is expected to apply also to the solutions for R = 1, 10, 50 in Figure 4(a)-(c). Further the influence of the finiteness of the computational domain is seen to be negligible over the bulk of the solution. As shown in Figure 4(d) no visible change in the results is produced by increasing the values of ξ_∞, η_∞ from 8, 4 respectively to 10, 5 respectively, which corresponds to increasing the extent of the computational domain from $-8 \leqslant x \leqslant 32$ to $-12.5 \leqslant x \leqslant 50$ along the x-axis. Indeed the resultant change in ζ_W is confined in general to the fourth significant figure.

Comparisons between the numerical solutions near the start and finish of the injection, $(\xi, \eta) \rightarrow (1,0)$ and $((2h+1)^{1/2}, 0)$, and the corresponding local analysis of (2.7)-(2.13) also prove fairly affirmative. Specifically, the values of Q_S and Q_F, where

$$Q_S = -\frac{3}{2h^2}(-V_W h + 2\psi_2) - \frac{1}{2}J_2\zeta_2, \tag{4.1a}$$

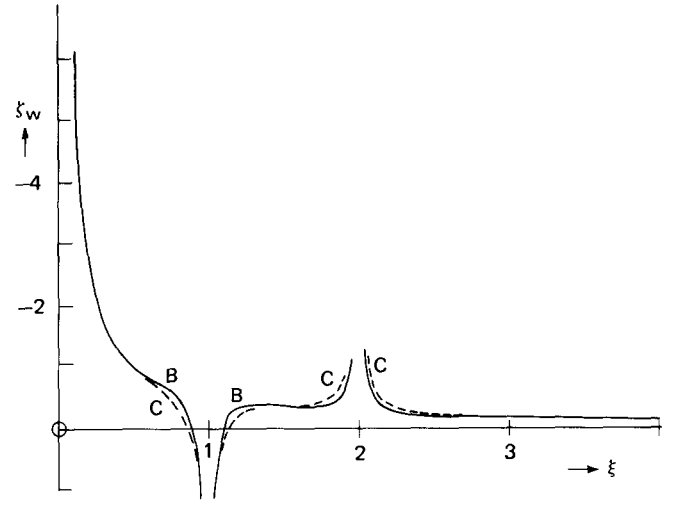
ζ_w
−4
−2
B
C
B
C
C
1
2
3
ξ

4a.

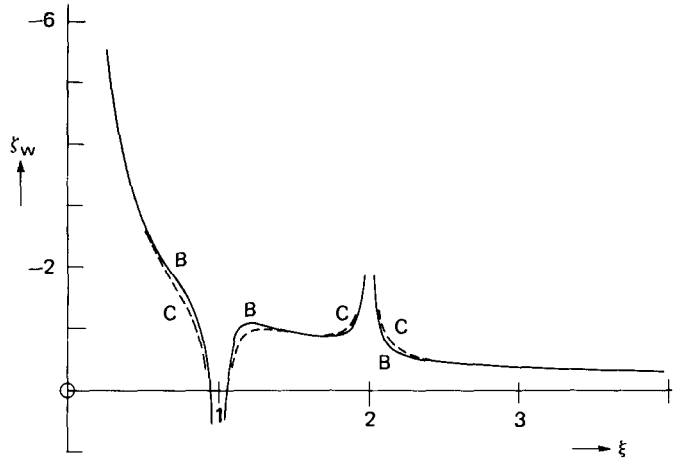
−6
ζ_w
−2
B
C
B
C
C
B
1
2
3
ξ

4b.

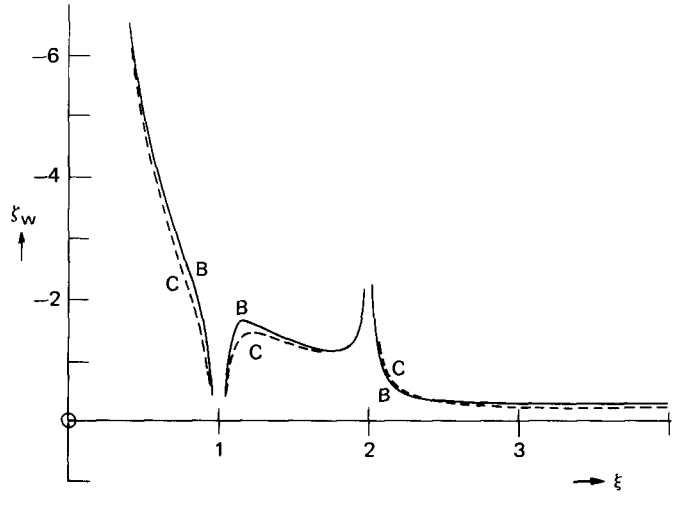
−6
−4
ζ_w
−2
C
B
B
C
C
B
1
2
3
ξ

4c.

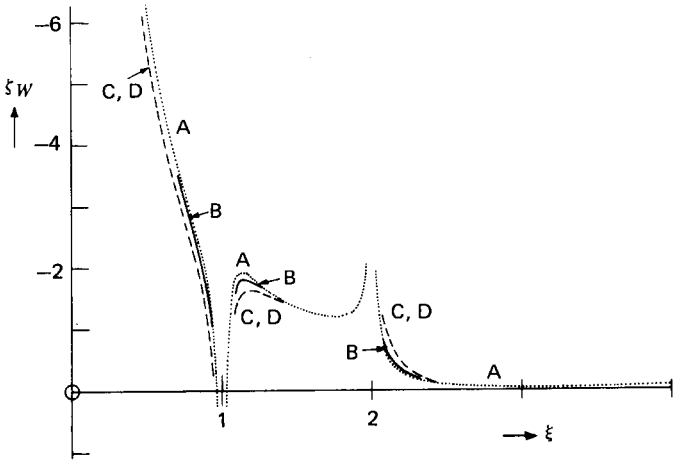

Figure 4. The numerical solutions obtained when $V_W = 0.2$, $L = 1.5$ for the wall vorticity ζ_W as a function of $\xi = x^2/2$: (a) $R = 1$, (b) $R = 10$, (c) $R = 50$, (d) $R = 100$. Here $h = 1/30$, $\xi_\infty = 8$, $\eta_\infty = 4$ for the solutions marked A; $h = 1/20$, $\xi_\infty = 8$, $\eta_\infty = 4$ for B; $h = 1/10$, $\xi_\infty = 8$, $\eta_\infty = 4$ for C; $h = 1/10$, $\xi_\infty = 10$, $\eta_\infty = 5$ for D. Where any two solutions are indistinguishable graphically only the finer grid solution is shown.

$$(2L+1)Q_F = -\frac{3}{2h^2}(V_W h + 2\psi_2 + 2V_W L) - \frac{1}{2}J_2\zeta_2, \tag{4.1b}$$

were calculated from the converged numerical solutions. In (4.1a,b) the subscripts 2 refer to evaluation at $\xi = 1$, $\eta = h$ and at $\xi = (2L+1) = 2$, $\xi = h$ respectively. We note incidentally that at first sight the values of Q_S and Q_F would seem to give numerical estimates for the wall vorticity at the start and finish of the injection, according to (3.8). In fact, of course, Q_S and Q_F are not employed in the numerical treatment at all since they are singular in the full solution ($h \to 0$) and instead of (4.1a,b) the rotated differencing referred to in Sec. 3 was adopted. However, the behaviour of Q_S as given by (4.1a) can be worked out from the local theory of Sec. 2, which predicts

$$Q_S \sim (3\pi + 8)V_W/2\pi h \tag{4.2}$$

as $h \to 0$, from the leading terms in (2.7) and the formulae in (2.8c,d). With $V_W = 0.2$, therefore, Sec. 2 predicts that

$$Q_S \sim \frac{0.555}{h} \text{ as } h \to 0. \tag{4.3a}$$

The corresponding prediction for Q_F obtained from the analogue of (2.7)-(2.13) near the finish of the injection is

$$Q_F \sim \frac{-0.277}{h} \text{ as } h \to 0. \tag{4.3b}$$

It follows that for (4.3a) to be satisfied the differences in the numerical results for Q_S calculated for $h = 1/10, 1/20$ should equal 5.55 if, as we hope, these two mesh widths are fine enough to be able to reproduce numerically the local behaviour (2.7). Similarly the differences in our numerical results for Q_F for $h = 1/10, 1/20$ should equal -2.77 according to (4.3b), if (2.7) is to be verified numerically. Tests on these predictions are presented in tables 1, 2 which give the calculated values of Q_S, Q_F for $R = 1, 10, 50, 100$ obtained from the two mesh widths $h = 1/10$, $1/20$ and, in the case $R = 100$, from $h = 1/30$ also; the predicted differences in Q_S, Q_F from the results for $h = 1/20, 1/30$ are again 5.55 and -2.77 according to (2.7) or (4.3a,b). Tables 1, 2 show that throughout the theoretical differences of 5.55 and -2.77 are reproduced reasonably well overall in the numerical solutions. The maximum deviation from the theoretical values is less than 2% even when $R = 100$. This tends to encourage the view that the numerical treatments of the singular points at the start and finish of the injection are consistent with (2.7) and reproduce (2.7) sufficiently accurately. Another point is that the behaviour of the numerical solutions for ζ_W near $\xi = 1$ and $\xi = 2$ in Figures 4(a)-(d) is also qualitatively in agreement with the local prediction (2.13) for $\xi \to 1$ and its counterpart for $\xi \to 2$. However the predictions (4.3a,b) with which quantitative comparisons have just been made provide a firmer test on the adequacy of the numerical treatments since they are much more singular than (2.13). For the dominant logarithmic term in (2.13) is of course of the same level of magnitude as the $O(1)$

TABLE 1

Numerical results for Q_S and comparisons with (4.3a)

R	(i)	(ii)	(iii)	(iv)	(v)
1	4.99	10.53	–	5.54	–
10	4.15	9.67	–	5.52	–
50	3.47	8.92	–	5.45	–
100	3.11	8.71	14.16	5.60	5.45

Columns (i)-(iii) give the values of Q_S obtained using the mesh widths $h = 1/10$, $1/20$, $1/30$ respectively, for the Reynolds numbers indicated. Columns (iv), (v) then give the values of the differences between the numbers in (i), (ii) and in (ii), (iii) respectively. The numerical values in (iv), (v) are to be compared with the prediction from (4.3a) of a value 5.55 for the limit $h \to 0$.

TABLE 2

Numerical results for Q_F and comparisons with (4.3b)

R	(i)	(ii)	(iii)	(iv)	(v)
1	−3.03	−5.80	–	−2.77	–
10	−3.39	−6.16	–	−2.77	–
50	−3.47	−6.25	–	−2.78	–
100	−3.46	−6.19	−8.92	−2.73	−2.73

Columns (i)-(v) are as in Table 1 but with Q_F replacing Q_S. The numerical values in (iv), (v) are to be compared with the prediction from (4.3b) of a value -2.77 for the limit $h \to 0$.

term there for all but a tiny range of small values of $|x - 1/2|$ or $|\xi - 1|$; further the arbitrariness in the constant A_1 of (2.11a,c) implies arbitrariness in the $O(1)$ term in (2.13) and hence the presence of an unknown constant factor multiplying $|x - 1/2|$ in (2.13) which again hinders the making of any firm numerical comparisons.

The dividing streamlines, $y = y_d(x)$ say, on which $\psi = 0$ in the $x-y$ plane were also calculated from the numerical solutions. They are shown in Figure 5 for the Reynolds numbers $R = 1$, 10, 100. These streamlines divide the injected fluid from the main streaming fluid and emanate from the plate at the separation position $x = x_{sep}$ where the skin friction or wall vorticity is zero. The position $x = x_{sep}$ always lies ahead of the start of the injection, in keeping again with the predictions of the local theory of Sec. 2, but x_{sep} increases with R over the range $R = 1$ to 100 studied although on the other hand the increase in x_{sep} when R is increased from 50 to 100 is minimal (see also Figure 3). Further, at each value of $x > x_{sep}$ a decrease in the displacement of the dividing streamline from the plate results from any increase in R. This aspect is also in line with the asymptotic form of the dividing stream line derived from the downstream behaviour (2.6) and the boundary condition (2.4d) which imply that

$$y_d(x) \sim \left(\frac{2V_W L}{\lambda R}\right)^{1/2} x^{1/4} \quad \text{as} \quad x \to \infty \tag{4.4}$$

where $\lambda = f_B''(0) = 0.33206$. Comparisons of the numerical results with the asymptote (4.4) are given in Figure 5 and prove reasonably satisfactory even for values of x in the range 3–4 shown provided allowance is made for the unknown origin shift implicit in (4.4).

The results for ζ_W and ψ in Figures 4, 5 all seem sensible physically and have certain interesting features. Notably the separation position $x = x_{sep}$ and reattachment position $x = x_{reatt}$, at which $\zeta_W = 0$, both tend to move closer to the starting point of the injection $x = x_s$ as the Reynolds number (R) increases (Figure 4(a)-(d)), although the change in x_{sep} as R is increased from 50 to 100 is small. There is certainly no conclusive sign yet for large R of any large scale separation upstream of the injection such as would be implied by the analogue for incompressible

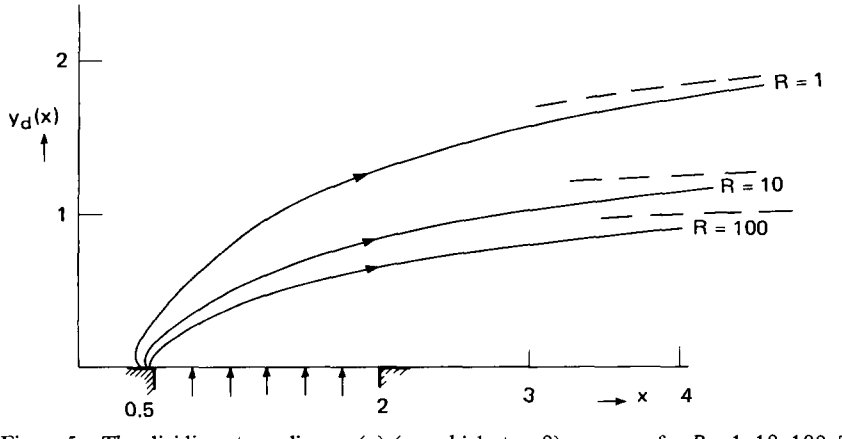

Figure 5. The dividing streamline $y_d(x)$ (on which $\psi = 0$) versus x, for $R = 1$, 10, 100. The dashed lines indicate the corresponding asymptotes (4.4) with a shift in the origin of $y_d(x)$ in each case. The hatching indicates the start and finish of the injection.

fluid flow of the supersonic flow theory of Smith and Stewartson [22] for high Reynolds numbers. Indeed, such a theory would imply that the separation point $x = x_{sep}$ approaches the leading edge $x = 0+$ in the limit as $R \to \infty$; the theory is the subject of a current investigation by Drs F. T. Smith and P. W. Duck, incidentally. Some evidence of significant upstream separation has been found experimentally in the incompressible case however (Smith [31]), but at much higher Reynolds numbers than those of the present computations. On the other hand there is a clear tendency for the local maximum of the wall vorticity beyond the finish of the injection to approach zero as the Reynolds number is increased in Figure 4(a)-(d). This bears some resemblance to the numerical results for asymptotically high Reynolds number flow of Napolitano and Messick [36] whose work suggested that significant separation may first occur downstream rather than upstream of the injection. Their triple-deck (Stewartson [23], Messiter [24]) injection problem has a much different context from ours, of course, but other trends of the present solutions are also akin to their results. The variations of the wall vorticity for increasing R, for instance, are not dissimilar to their calculated variations or indeed to the linearized solutions of the triple-deck problem as described by Smith [21] and Napolitano and Messick [36]. The accentuation of the local maximum of $-\zeta_W$ just beyond the start of the injection and the decreased slope of $-\zeta_W$ immediately after that, for $R = 100$, seem characteristic of the high Reynolds number theory (Napolitano and Messick [36], Smith and Stewartson [16], [22]). Here it seems worth mentioning also that the occurrence of the separation significantly far ahead of the start of the injection in the case $R = 1$ (Figures 4(a), 5) might suggest the occurrence of a Stokes flow separation upstream in the Stokes limit $R \to 0+$, which would be of some interest. We would re-emphasize finally however that the local analysis of (2.7)-(2.13) shows, and our calculations verify (Figures 4-5), that separation in the sense of flow reversal always takes place upstream of the injection for all nonzero Reynolds numbers R. Whether this upstream separation remains quite close to the start of the injection with further increases in R beyond 100 or instead leads to a large scale separation process significantly far ahead of the injection, of the type considered by Smith and Stewartson [22], Sychev [33] and Smith [34], remains to be seen. No successful attempts at obtaining numerical solutions for values of R greater than 100 have so far been made.

5. Further comments

The checks applied to the numerical work and described in Secs. 3, 4 above all seem to prove satisfactory and tend to suggest that the numerical results obtained here are reasonably accurate. The checks include allowance for the influences of mesh spacing (Figures 4(a)-(d)) and of the placing for the outer boundaries of the computational domain (Figure 4(d)), as well as of the treatments applied to the singular points at the leading edge (Figure 3) and at the ends of the injection (Tables 1, 2). In particular the agreement found between the present numerical solutions and the local analysis of Sec. 2, which leads to the predictions (4.3a,b), is especially encouraging since the treatment of singular points in the calculation of any flowfield is always an issue of concern and is often the subject of much scepticism. There would seem to be few real grounds for such scepticism in the context of the treatment of the singular points in the present injection problem.

The fluid dynamical aspects of the local theory of Sec. 2 combined with the calculated results just presented in Sec. 4 have certain intriguing qualities. Specifically they lend some support to both the prospects raised in the introduction concerning the occurrence of separation in the high Reynolds number regime. For on the one hand Sec. 2 shows that separation ahead of the injection is bound to occur because of the positive infinite value of the wall vorticity at the start of the injection and the calculations fully confirm this. On the other hand the separation point moves marginally closer to the start of the injection as the Reynolds number R increases, at least in the range $1 \leqslant R \leqslant 100$ studied numerically here, while not far downstream of the injection the wall vorticity has a tendency to approach zero with increasing R, thus suggesting the possibility of the onset of a downstream separation. It may be, in fact, that significant separation both upstream and downstream of the injection is inevitable at higher Reynolds numbers. To help decide this and other issues regarding the high Reynolds number laminar flow properties of the incompressible injection problem further accurate numerical solutions of the Navier-Stokes equations with separation may well provide valuable guidance towards extending the current relatively limited understanding of the asymptotic structure of the solution. It is hoped that such further numerical solutions will be obtainable by the present methods because of the advantage gained from employing the augmented centred-differencing technique of Dennis [1] and Dennis and Hudson [2]. Again, we envisage that the calculations presented in this paper for the range $1 \leqslant R \leqslant 100$ may themselves provide the kind of quantitative results against which the relevance, if not the theoretical validity, of any future asymptotic theory on the subject can be judged.

Acknowledgement

One of us (F.T.S.) is grateful to the Natural Sciences & Engineering Research Council of Canada for financial support in the early stages of this work.

REFERENCES

[1] Dennis, S. C. R., Finite differences associated with second-order differential equations, *Quart. J. Mech. Appl. Math.* 13 (1960) 487-507.
[2] Dennis, S. C. R. and Hudson, J. D., A difference method for solving the Navier-Stokes equations, *Proc. 1st. Int. Conf. on Num. Meth. in Lam. & Turb. Flow*, Univ. Coll. Swansea, U.K. (July 1978), Pentech Press, London, England (1978) 69-80.
[3] Spence, D. A., The lift coefficient of a thin jet-flapped wing, *Proc. Roy. Soc.* A238 (1956) 46-68.
[4] Spence, D. A., The lift on a thin aerofoil with a jet-augmented flap, *Aeron. Quart.*, Aug. (1958) 287-299.
[5] Stratford, B. S., Early thoughts on the jet flap, *Aeron. Quart.*, Feb. (1956), VII.
[6] Stratford, B. S., Mixing and the jet flap, *Aeron. Quart.*, May (1956), VIII.
[7] Leamon, R. G. and Plotkin, A., An improved solution of the two-dimensional jet-flapped airfoil problem, *AIAA J.* 9 (1972) 631-635.
[8] Sato, J., Discrete vortex method of two-dimensional jet flaps, *AIAA J.* 11 (1973) 968-973.
[9] Ives, D. C. and Melnik, R. E., Numerical calculation of the compressible flow over an airfoil with a jet flap, *AIAA Paper* (1974), no. 74-542.
[10] O'Mahoney, R. and Smith, F. T., Calculation of the flow past an aerofoil with a jet flap, *Aeron. Quart.*, Feb. (1978) 43-59.

[11] Hartunian, R. A. and Spencer, D. J., Visualization technique for massive blowing studies, *AIAA J.* 4 (1966) 1305-1307.
[12] Hartunian, R. A. and Spencer, D. J., Experimental results for massive blowing studies, *AIAA J.* 5 (1967) 1397-1401.
[13] Fernandez, F. L. and Zukoski, E. E., Experiments in supersonic turbulent flow with large distributed injection, *AIAA J.* 7 (1969) 1759-1767.
[14] Goldstein, R. J., Film cooling, *Adv. in Heat Transfer* 7 (1971) 321-379.
[15] Inger, G. R. and Gaitatzes, G. A., Strong blowing into supersonic laminar flows round two-dimensional and axisymmetric bodies, *AIAA J.* 9 (1971) 436-443.
[16] Smith, F. T. and Stewartson, K., On slot-injection into a supersonic laminar boundary layer, *Proc. Roy. Soc.* A332 (1973) 1-22.
[17] Pretsch, J., Die laminare Grenzschichte bei starken absaugen und ausblasen, *Unter. Mitt. Deut. Luft* (1944) Rep. 3091.
[18] Emmons, H. W. and Leigh, D. C., Tabulation of the Blasius function with blowing and suction, *A.R.C.* (1954) Current paper no. 157, London, U.K..
[19] Diver, C. and Stewartson, K., On moderate injection into a separated supersonic boundary layer with reattachment, *J. Fluid Mech.* 88 (1978) 115-132.
[20] Catherall, D., Stewartson, K. and Williams, P. G., Viscous flow past a flat plate with uniform injection, *Proc. Roy. Soc.* A284 (1965) 370-396.
[21] Smith, F. T., A theoretical, experimental and numerical investigation of uniform injection from a flat plate into a uniform stream, D. Phil. Thesis (1972), Oxford University, U.K..
[22] Smith, F. T. and Stewartson, K., Plate-injection into a separated supersonic boundary layer, *J. Fluid Mech.* 58 (1973) 143-159.
[23] Stewartson, K., Multistructured boundary layers on flat plates and related bodies, *Adv. in Appl. Mech.* 14 (1974) 145-239.
[24] Messiter, A. F., Boundary layer separation, *Proc. 8th U.S. Nat. Appl. Math. Congress* (1979), Los Angeles, California, U.S.A..
[25] Stewartson, K., Plate-injection into a separated supersonic boundary layer. Part 2, The transition regions, *J. Fluid. Mech.* 62 (1974) 289-304.
[26] Stewartson, K. and Williams, P. G., Self-induced separation, *Proc. Roy. Soc.* A312 (1969) 181-206.
[27] Messiter, A. F., Hough, G. R. and Feo, A., Base pressure in laminar supersonic flow, *J. Fluid Mech.* 60 (1973) 605-624.
[28] Burggraf, O. R., Asymptotic theory of separation and reattachment of a laminar boundary layer on a compression ramp, *AGARD* paper no. 168 on flow separation (1975), Gottingen.
[29] Rizzetta, D. P., Burggraf, O. R. and Jenson, R., Triple-deck solutions for viscous supersonic and hypersonic flow past corners, *J. Fluid Mech.* 89 (1978) 535-552.
[30] Wallace, J. and Kemp, N. H., Similarity solutions to the massive blowing problem, *AIAA J.* 7 (1969) 1527-1523.
[31] Smith, F. T., On strong blowing into an incompressible airstream, *J. Fluid Mech.* 60 (1973) 241-255.
[32] Cole, J. D. and Aroesty, J., The blowhard problem – inviscid flows with surface injection, *Int. J. Heat & Mass Transfer* 11 (1968) 1167-1183.
[33] Sychev, V. V., Concerning laminar separation, *Izv. Akad. Nauk. SSSR, Mekh. Zh. Gaza* 3 (1972) 47-59.
[34] Smith, F. T., The laminar separation of an incompressible fluid streaming past a smooth surface, *Proc. Roy. Soc.* A356 (1977) 443-463.
[35] Smith, F. T., The laminar flow of an incompressible fluid past a bluff body: the separation, reattachment, eddy properties and drag, *J. Fluid Mech.* 92 (1979) 171-205.
[36] Napolitano, M. and Messick, R. E., On strong slot injection into a subsonic laminar boundary layer, *Computers & Fluids* 8 (1980) 199-212.
[37] Dennis, S. C. R. and Smith, F. T., Steady flow through a channel with a symmetrical constriction in the form of a step, *Proc. Roy. Soc.* A372 (1980) 393-414.
[38] Smith, F. T., The separating flow through a severely constricted symmetric tube, *J. Fluid Mech.* 90 (1979) 725-754.
[39] Dean, W. R. and Montagnon, P. E., On the steady motion of viscous liquid in a corner, *Proc. Camb. Phil. Soc.* 45 (1949) 389-394.
[40] Moffatt, H. K., Viscous and resistive eddies near a sharp corner, *J. Fluid Mech.* 18 (1964) 1-18.
[41] Walsh, J. D. M., Steady viscous flow past a parabolic cylinder, Ph. D. Thesis (1973), University of Western Ontario, Canada.

[42] Woods, L. C., A note on the numerical solution of fourth order differential equations, *Aero. Quart.* 5 (1954) 176-184.
[43] Van de Vooren, A. I., and Dijkstra, D., The Navier-Stokes solution for laminar flow past a semi-infinite flat plate, *J. Eng. Math.* 4 (1970) 9-27.
[44] Van de Vooren, A. I., and Veldeman, A. E. P., Incompressible viscous flow near the leading edge of a flat plate admitting slip, *J. Eng. Math.* 9 (1975) 235-249.